Biochemical and Biophysical Research Communications 839 (2026) 154685

Contents lists available at ScienceDirect

Biochemical and Biophysical Research Communications

journal homepage: www.elsevier.com/locate/ybbrc

DYRK1B overexpression promotes senescence-like transcriptional and secretory programs in A549 lung cancer cells

Gerrit Wilms [a], Aaron Babendreyer [b], Justyna Wozniak [c], Florian Kraft [d], Walter Becker [a,*]

[a] Institute of Pharmacology and Toxicology, RWTH Aachen University, Aachen, 52074, Germany
[b] Institute of Molecular Pharmacology, RWTH Aachen University, Aachen, 52074, Germany
[c] Institute of Clinical Pharmacology, University Hospital of RWTH Aachen, Aachen, 52074, Germany
[d] Medical Faculty, Center for Human Genetics and Genomic Medicine, RWTH University Aachen, Aachen, 52074, Germany

ARTICLE INFO

Keywords:
DYRK1B
A549
Lung adenocarcinoma
Phenotypic plasticity
Cancer cell senescence
Senescence-associated secretory phenotype (SASP)
Epithelial–mesenchymal transition (EMT)

ABSTRACT

The dual-specificity tyrosine-regulated kinase DYRK1B is frequently expressed at elevated levels in solid tumors and has been implicated in cancer cell survival, therapy resistance, and cell cycle arrest. While DYRK1B is best known for maintaining quiescence, its broader impact on cancer cell phenotypic plasticity remains incompletely understood. Using a doxycycline-inducible A549 lung adenocarcinoma model, we show that sustained overexpression of catalytically active DYRK1B induces senescence-related phenotypic changes. DYRK1B overexpression led to increased senescence-associated β-galactosidase activity, cell enlargement and granularity, and robust induction of the cyclin-dependent kinase inhibitor $p21^{Waf1/Cip1}$. RNA-sequencing revealed extensive transcriptional reprogramming, with strong overlap to established cellular senescence signatures. Gene set enrichment analysis further identified suppression of E2F target genes, consistent with durable proliferation arrest. Senescence-associated secretory phenotype (SASP) components, including PAI-1 (SERPINE1), CCL2, IGFBP7, were significantly upregulated at both mRNA and protein levels. These effects were not observed with a kinase-impaired DYRK1B mutant. Gene set enrichment analysis further identified enrichment of epithelial–mesenchymal transition (EMT) transcriptional programs, consistent with EMT-associated phenotypic effects of DYRK1B overexpression that we have reported previously. These findings identify DYRK1B as an inducer of senescence-like transcriptional and secretory programs when expressed at elevated levels in A549 lung cancer cells in vitro. Although currently speculative and awaiting in vivo validation, we hypothesize that DYRK1B-induced senescence might contribute to tumor cell persistence and therapy resistance, highlighting DYRK1B as a potential target for modulating cancer cell plasticity and senescence-associated phenotypes.

1. Background

Dual-specificity tyrosine-regulated kinases (DYRKs) are an evolutionarily conserved family of protein kinases that mediate cellular stress responses across a wide range of organisms, including yeasts (*S. cerevisiae*, *C. albicans*), slime molds, fungi, plants, and mammals [1 2 3]. Typically, DYRK kinases function as negative regulators of the cell cycle, promoting cell survival under adverse conditions such as nutrient deprivation, oxidative stress, and DNA damage.

Among the human members of the DYRK family, DYRK1B has emerged as a key survival kinase in cancer cells. It is frequently upregulated in various cancers and has been shown to enhance resistance to chemo- and radiotherapy [4 5 6 7]. DYRK1B exerts its protective effects by inducing cell cycle exit [8 9], upregulating the expression of antioxidant genes [10,11], and facilitating DNA damage repair [12]. Notably, inactivation of DYRK1B, either genetically or pharmacologically, can sensitize cancer cells to cytotoxic agents [5].

While previous studies have primarily emphasized the role of DYRK1B in maintaining cancer cells in a quiescent, non-proliferative state, we have recently characterized phenotypic changes induced by elevated DYRK1B expression in A549 lung adenocarcinoma cells [13]. These include pronounced morphological alterations, reorganization of the actin cytoskeleton, enhanced migratory capacity, and transcriptional reprogramming suggestive of epithelial-to-mesenchymal

* Corresponding author.
E-mail address: walter.becker@post.rwth-aachen.de (W. Becker).

https://doi.org/10.1016/j.bbrc.2026.154685
Received 29 July 2026; Received in revised form 1 September 2026; Accepted 3 October 2026
Available online 6 October 2026
0006-291X/© 2026 The Authors. Published by Elsevier Inc. This is an open access article under the CC BY license (http://creativecommons.org/licenses/by/4.0/).
Open access funding enabled and organized by Projekt DEAL.

transition (EMT). Specifically, DYRK1B overexpression increases the expression of EMT-associated transcription factors SNAIL and SLUG, key regulators of this phenotypic switch. EMT contributes to cancer cell plasticity, endowing epithelial cells with mesenchymal traits, enhanced survival, and metastatic potential [14 15].

Another stress-associated phenotypic adaptation linked to cell cycle exit is cellular senescence [16 17]. Interestingly, DYRK1B expression was recently reported to increase in endothelial cells undergoing senescence [18]. Furthermore, the closely related kinase DYRK1A contributes to oncogene-induced senescence in hTERT-immortalized BJ fibroblasts [19], and mediates senescence induction in castration-resistant prostate cancer [20].

In this study, we further investigate the consequences of DYRK1B overexpression in A549 cells. Building on our previous findings [13] that DYRK1B-overexpressing cells exhibit an enlarged, flattened morphology and increased cytoplasmic granularity - features reminiscent of senescent cells - we evaluated multiple hallmarks of cellular senescence to define the downstream effects of elevated DYRK1B levels in A549 cells. Specifically, we examined the expression of key senescence-associated biomarkers, performed global transcriptome analysis, and demonstrated that DYRK1B overexpressing cells secrete multiple components of the senescence-associated secretory phenotype (SASP).

2. Methods

2.1. Materials

Critical research reagents and tools (antibodies, commercial kits and chemicals) are specified in the supplementary information.

2.2. Cell culture

Stable A549 sublines for tetracycline-inducible overexpression of $DYRK1B^{WT}$ or $DYRK1B^{Y273F}$ were generated with the help of a lentiviral vector system and have been characterized previously [13]. All experiments in this study were performed with an A549 tetON-$DYRK1B^{WT}$ cell pool formed from 10 positive cell clones. Cells were maintained in Gibco DMEM/F-12 medium supplemented with 10% fetal bovine serum in a 37°C incubator with a humidified atmosphere of 5% CO_2. Cells were split using Accutase and routinely tested for mycoplasma contamination. Doxycycline was used at a final concentration of 2 μg/mL to induce the expression of DYRK1B.

2.3. SA-β-gal staining

Cells were fixed and stained for SA-ß-gal activity using a commercial kit (CST, Danvers, MA, USA; #9860). X-Gal stock (20 mg/ml) was prepared in DMSO. Staining proceeded for 24 h at 37°C. Cells were mounted and evaluated by bright field microscopy (Axiovert 135, Carl Zeiss, Jena, Deutschland).

2.4. FACS

A549-tetON cells were cultured for seven days in the presence or absence of doxycycline (2 μg/mL) to induce co-overexpression of GFP and either $DYRK1B^{WT}$ or $DYRK1B^{Y273F}$. After harvesting, induced and non-induced cell populations were combined in a FACS tube and centrifuged for 5 min at 300 × g and 4°C. The pooled cells were washed with 1 ml PBS, fixed for 5 min in 600 μL 2% paraformaldehyde at room temperature, washed again with PBS, and finally resuspended in 400 μL PBS. Both cell pools were analyzed using an LSRFortessa flow cytometer for GFP positivity, forward scatter (FSC) and side scatter (SSC). $DYRK1B^{WT}$ and $DYRK1B^{Y273F}$ overexpressing and non-overexpressing cell were distinguished based on GFP fluorescence. Data were analyzed using FlowJo software version 10.1.

2.5. Western blot analysis

For Western blot experiments, cells were seeded at low density and cultured in 6-well plates for 7 days. Cells were washed with ice cold PBS, and lysed for 30 min at 4°C in a non-denaturing lysis buffer (20 mM HEPES pH 7.4, 150 mM NaCl, 2 mM EDTA, 1% Igepal CA 630. The buffer was supplemented with phosphatase and protease inhibitors (1 mM Na_3VO_4, 1 mM PMSF, 10 μg/mL aprotinin,4 μg/mL pepstatin and 16 μg/mL leupeptin). Lysates were cleared by centrifugation, and equal amounts of protein were then subjected to immunoblot analysis. Chemiluminescence signals were captured using a CCD imager (Fujifilm LAS-3000), and bands intensities were measured using Multi Gauge software (Fujifilm) with background subtraction. To account for inter-experimental variation, individual band intensities were normalized to the sum of all relevant data points within each independent replicate [21].

2.6. ELISA

ELISA were performed with the conditioned media taken from the same wells of A549-tetON cells that were analyzed by immunoblotting. After four days, the medium was replaced with fresh medium with or without doxycycline, allowing secreted proteins to accumulate for an additional three days. After seven days total incubation, culture supernatants were collected, frozen at −80°C, and analyzed for secreted PAI-1, CCL2, and IGFBP7 using commercial ELISA kits (supplemental material, Table S2).

2.7. RNA-seq analysis

Total RNA was isolated using commercial extraction kits as detailed in Table S2. RNA quantity and quality were assessed using an Agilent TapeStation system and a QFX fluorometer (Denovix). RNA-seq libraries were generated with the QuantSeq FWD V2 library preparation kit (Lexogen, and sequencing was carried out on an Illumina NovaSeq 6000 platform using single-end reads (1 × 118 cycles), yielding approximately 8–10 million reads per sample.

Base calling and demultiplexing were performed with *bcl_convert*, and sequencing reads were exported in FASTQ format. Reads were aligned to the human reference genome GRCh38p14 using STAR Aligner [22], and gene-level counts were obtained accordingly. Downstream analysis and visualization were conducted using the BioJupies platform with default settings [23]. Pairwise comparisons between experimental groups were used to identify differentially expressed genes. BioJupies applies the limma framework [24], in which raw read counts are converted to counts per million (CPM) and normalized using the *voom* method. Gene-wise linear models were fitted, and differential expression was estimated using an empirical Bayes approach with variance shrinkage, followed by statistical assessment using moderated t-statistics.

2.8. GSEA

Gene set enrichment analysis (GSEA) [25] was performed using the Broad Institute GSEA desktop application (version 4.4.0) with default parameters. Expression data comparing $DYRK1B^{WT}$ overexpressing and non-induced cells] were used to generate a ranked list of 12,720 genes ordered by fold change between the two phenotypic groups. The analysis was run against the Hallmark gene set collection from Human MSigDB (v2025.1.Hs) [26] and against the cellular senescence signature sets of genes that classified as over- or underexpressed in the CellAge database (CellAge Build 3, released 23/04/2023). Enrichment scores were calculated using the weighted Kolmogorov–Smirnov–like statistic, and statistical significance was estimated by permutation testing with default settings, controlling for multiple testing by the false discovery rate (FDR).

2.9. Statistics

Statistical analyses were performed using two-way analysis of variance (ANOVA) based on linear mixed-effects models implemented with the PROC GLIMMIX procedure (SAS 9.4, SAS Institute Inc., Cary, NC, USA). Model assumptions were evaluated by inspection of residuals, and normality was assessed using the Shapiro–Wilk test. Model fit was assessed using the Akaike Information Criterion (AIC) and Bayesian Information Criterion (BIC). Where appropriate, p-values were adjusted for multiple comparisons using the Bonferroni correction. A p-value < 0.05 was considered statistically significant, with significant differences indicated by asterisks. Statistical analyses of the RNA-seq data are described above.

3. Results

3.1. Overexpression of DYRK1B induces senescence-like phenotypic changes in A549 cells

To investigate the effects of elevated DYRK1B levels, we utilized a previously established A549 cell model with doxycycline-inducible co-overexpression of GFP and wild-type DYRK1B (A549-tetON GFP-T2A-DYRK1B^{WT}; [13]). As a control, we employed a corresponding cell line expressing DYRK1B^{Y273F}, a catalytically impaired mutant carrying a substitution at the autophosphorylation site. Both cell lines express wild-type and mutant DYRK1B at comparable levels, ensuring that observed phenotypic differences are attributable to kinase activity rather than expression level [13]. Induced overexpression of DYRK1-B^{Y273F} controls both for unspecific effects of doxycycline exposure, and mass-action effects of protein overexpression, and for kinase-independent scaffolding functions of DYRK1B, such as sequestering interacting partners or disrupting endogenous protein complexes.

Cells were cultured in the presence of doxycycline for seven days to induce transgene expression and subsequently stained for senescence-associated β-galactosidase (SA-β-gal) activity, a classical marker of cellular senescence [27]. As shown in Fig. 1A, overexpression of wild type DYRK1B but not DYRK1B^{Y273F} led to the appearance of SA-β-gal positive cells. As we have previously reported, DYRK1B^{WT} overexpressing cells were also characterized by pronounced morphological alterations, including cell enlargement and loss of defined colony borders [13]. These changes closely resembled those observed in published studies of doxorubicin- or radiation-induced senescence in A549 cells [28 29].

For comparison with a well characterized model of cancer cell senescence, A549 cells were treated with 100 nM doxorubicin to induce DNA damage-mediated senescence [30]. Doxorubicin treatment resulted in similar morphological alterations and widespread SA-β-gal staining (Fig. 1B).

Two hallmark features of senescent cells - cellular enlargement and increased granularity - can be assessed by flow cytometry [27 31]. Forward scatter (FSC) provides a measure of cell size, while side scatter (SSC) reflects cellular granularity, mainly indicative of increased

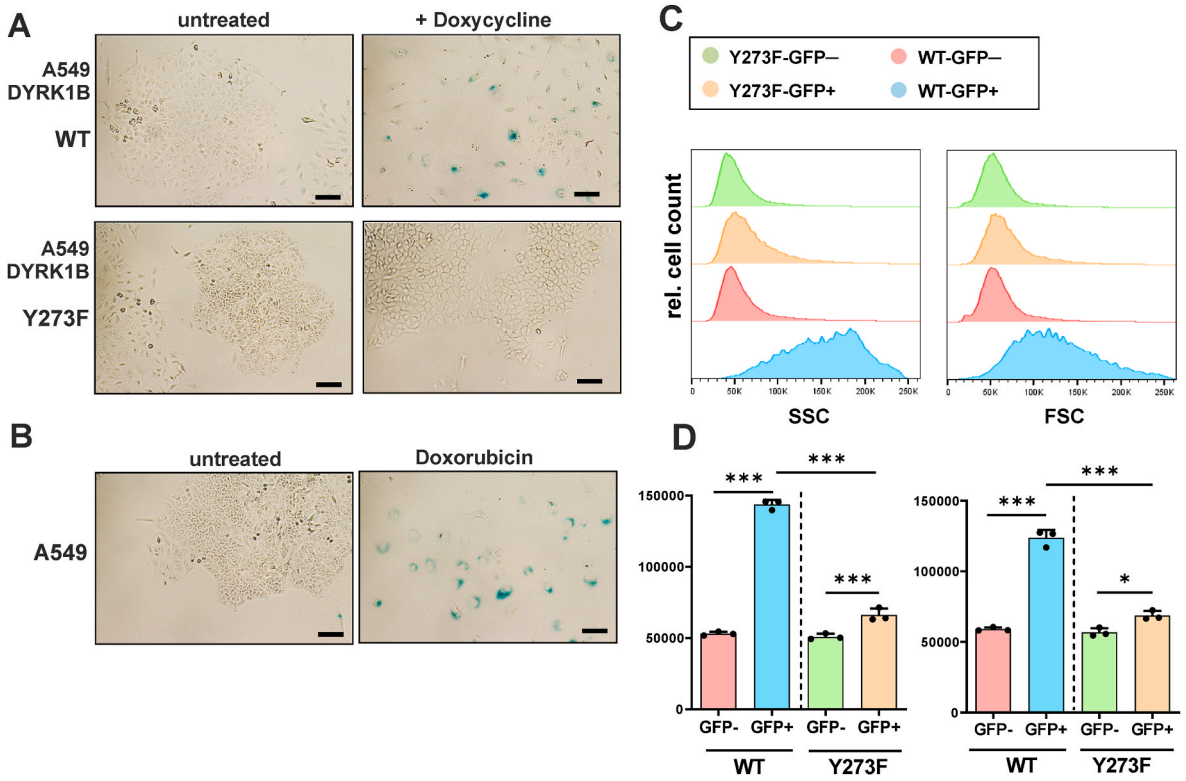


Fig. 1. DYRK1B overexpression induces features of cellular senescent cells. A, SA-β-galactosidase activity. A549 tetON DYRK1B cells were cultured for seven days in the presence or absence of doxycycline to induce overexpression of DYRK1B^{WT} or DYRK1B^{Y273F}. Representative images of cells stained for SA-ß-gal-stained cells are shown; senescent cells appear blue. The morphologic changes of DYRK1B-overexpressing A549 cells have been characterized in our previous report [13]. **B,** A549 cells were treated with doxorubicin (100 nM) for 7 d as a positive control for senescence induction. Images in panel **A** and **B** are representative of n = 3 independent experiments, with at least five fields imaged per condition. Scale bar, 100 μm **C** and **D**, FACS analysis of cell size and granularity. A549 tetON cells were cultured for 7 d with and without induced overexpression of DYRK1B^{WT} or DYRK1B^{Y273F}. To minimize variability, induced and uninduced cell populations were mixed prior to analysis and distinguished based on GFP expression. GFP-positive and GFP-negative cell populations were analyzed for forward scatter (FSC, reflecting cell size) and side scatter (SSC, reflecting cellular granularity). **C**, Representative histograms show the frequency distribution of GFP-positive and -negative DYRK1B^{WT} and DYRK1B^{Y273F} cell populations. **D**, Quantification of FSC and SSC intensities (geometric means) from n = 3 independent experiments (mean ± SD). Statistical significance relative to control cells is indicated (*$p < 0.05$, **$p < 0.01$, ***$p < 0.001$). (For interpretation of the references to colour in this figure legend, the reader is referred to the Web version of this article.)

content of lysosomes, protein aggregates, and exocytotic vesicles.

Long-term induction of DYRK1B increased FSC and SSC, proxy measures of size and granularity under our acquisition conditions (Fig. 1C). Notably, nearly all GFP-positive cells (indicating DYRK1B expression) exhibited both increased granularity and enlarged size, further supporting a role for DYRK1B in promoting senescence-like cellular remodeling. In contrast, these parameters were minimally changed in cells overexpressing the catalytically inactive DYRK1B^{Y273F} mutant. This small, but significant effect is likely due the residual activity of this point mutant (~2% of wild type DYRK1B [32]).

3.2. DYRK1B overexpression induces senescence-associated gene expression

Next we examined the expression of p21$^{Waf1/Cip1}$ and PAI-1 (plasminogen activator inhibitor-1), two well-established biomarkers and functional mediators of cellular senescence [27 33 34]. Overexpression of DYRK1B^{WT} caused a time-dependent increase in the levels of both p21$^{Waf1/Cip1}$ and PAI-1 over time, with maximal levels after 7 days of induction. In contrast, overexpression of the kinase-inactive mutant DYRK1B^{Y273F} had no significant effect on the expression of either gene, underscoring the requirement for DYRK1B's catalytic activity in mediating these senescence-associated transcriptional changes.

3.3. Transcriptomic profiling

To characterize the global transcriptional response to DYRK1B overexpression, we performed RNA-seq analysis in A549-tetON-DYRK1B cells. This analysis identified 2161 significantly upregulated genes (742 with $\log_2FC > 1.5$) and 1704 significantly downregulated genes (316 with $\log_2FC < -1.5$) at a false discovery rate (FDR) < 0.05 (Fig. 3A and B). Notably, *CDKN1A* (encoding p21$^{Waf1/Cip1}$) and *SERPINE1* (encoding PAI-1) were identified among the set of genes with strongly and significantly increased mRNA levels. In addition, several components of the SASP - including *CCL2* (chemokine (C-C motif) ligand 2, also known as monocyte chemoattractant protein 1, MCP-1), *IGFBP7* (insulin-like growth factor-binding protein 7), and *TGFB1* - were significantly induced, consistent with a senescence-like phenotype [27]. In contrast, overexpression of the kinase-impaired mutant DYRK1B^{Y273F} caused much weaker transcriptomic changes, suggesting that DYRK1B's catalytic activity is essential for driving the observed gene expression program.

To benchmark these transcriptomic changes against established senescence-associated gene sets, we leveraged the CellAge database, a compilation of genes that were found to be consistently over- and underexpressed in replicative senescence [35 36]. Of the 595 differentially expressed genes overlapping between our dataset and the CellAge reference, 85% of upregulated genes and 88% of downregulated genes matched the directionality of expression in the senescence reference signature (Fig. 3C). These findings demonstrate that DYRK1B overexpression induces transcriptional changes closely aligned with those in other models of cellular senescence.

To further characterize the biological processes associated with the gene expression changes observed in DYRK1B^{WT}-overexpressing cells, we performed Gene Set Enrichment Analysis (GSEA) [25]. For an unbiased assessment, we utilized the "Hallmark gene sets" from the Molecular Signatures Database (MSigDB), which comprise groups of genes that are coordinately expressed in well-defined biological states or processes [26]. Among the 50 hallmark gene sets, the strongest positive enrichment was observed for the "Epithelial–Mesenchymal Transition" (EMT) gene set (Fig. 3D), consistent with our previous finding that DYRK1B-overexpressing cells exhibit EMT-like features [13]. Conversely, the strongest negative enrichment was found for the "E2F targets" gene set (Fig. 3E), reflecting cell cycle arrest, also in agreement with our earlier observations [13].

Because the Hallmark collection does not include a gene set specifically representing the state of cellular senescence, we employed the CellAge signature gene lists to assess the enrichment of senescence-associated genes in DYRK1B^{WT}-overexpressing cells. This analysis revealed a strong enrichment of genes upregulated during senescence ("CellAge_up") among the transcripts increased in DYRK1B^{WT}-overexpressing cells (Fig. 3F). In contrast, genes typically downregulated in senescence ("CellAge_down") were significantly enriched among transcripts with reduced expression in DYRK1B-overexpressing cells (Fig. 3G). The normalized enrichment scores for the CellAge gene sets were comparable to those of the Hallmark EMT gene set, suggesting that DYRK1B induces phenotypic changes in A549 cells that encompass features of both EMT and cellular senescence. Strong positive enrichment was also observed with senescence-associated gene sets from other previous gene expression studies, including a recently established senescence-specific gene signature from which quiescence-associated genes were explicitly subtracted [37 38 39] (Suppl. Fig. S1).

Pathway enrichment analysis using the KEGG database further supports this conclusion. Among the most significantly upregulated pathways are "p53 signaling" and "proteoglycans in cancer," while "cell cycle" and "DNA replication" are among the most significantly downregulated (Suppl. Table S1). Importantly, these pathways also featured prominently in the CellAge senescence gene signature [36], reinforcing the link between DYRK1B activity and a senescence-associated transcriptional program.

3.4. DYRK1B overexpression induces secretion of SASP factors

A defining feature of senescent cells is the secretion of a broad range of bioactive molecules collectively referred to as the senescence-associated secretory phenotype (SASP). We therefore analyzed the secretion of selected SASP components (PAI-1, CCL2, IGFBP7) in conditioned media from DYRK1B-overexpressing A549 cells.

Secretion of PAI-1 was significantly increased after seven days of DYRK1B-WT overexpression (Fig. 4A), consistent with the corresponding rise in cellular protein abundance (Fig. 2) and mRNA expression (Fig. 3B). CCL2 levels were markedly elevated as early as three days post-induction (Fig. 4B). Importantly, overexpression of the kinase-inactive mutant DYRK1B^{Y273F} had no significant effect on the secretion of either PAI-1 or CCL2. Extracellular levels of IGFBP7 were significantly increased after seven days of DYRK1B^{WT} overexpression, but not upon expression of DYRK1B^{Y273F} (Fig. 4C), confirming that IGFBP7 upregulation depends on DYRK1B catalytic activity. Unexpectedly, basal secretion of IGFBP7 was substantially higher in uninduced A549 tetON DYRK1B^{Y273F} cells compared to the WT cell line, and these levels decreased upon induction of the mutant construct. While the precise mechanism underlying this observation remains to be fully elucidated, it is plausible that the DYRK1B^{Y273F} mutant exerts a dominant-negative effect. Specifically, the catalytically impaired protein may sequester an unknown substrate, a scaffolding protein, or another DYRK1B-interacting partner required for baseline IGFBP7 expression, thereby disrupting its normal regulatory network.

Nevertheless, taken together, the analysis of these secreted proteins indicates that sustained, catalytically active DYRK1B overexpression is associated with increased extracellular levels of canonical SASP components.

4. Discussion

Phenotypic plasticity - the ability of cancer cells to adopt diverse biological states - plays a critical role in enabling tumor cells to adapt to environmental stress and therapeutic challenges. Given the frequent upregulation of DYRK1B in solid tumors, we investigated its downstream effects on the cellular behavior of A549 lung cancer cells. Our findings demonstrate that DYRK1B overexpression not only promotes cell cycle exit [13] but also induces a spectrum of changes characteristic of cellular senescence [40 27]. These include (a) pronounced alterations

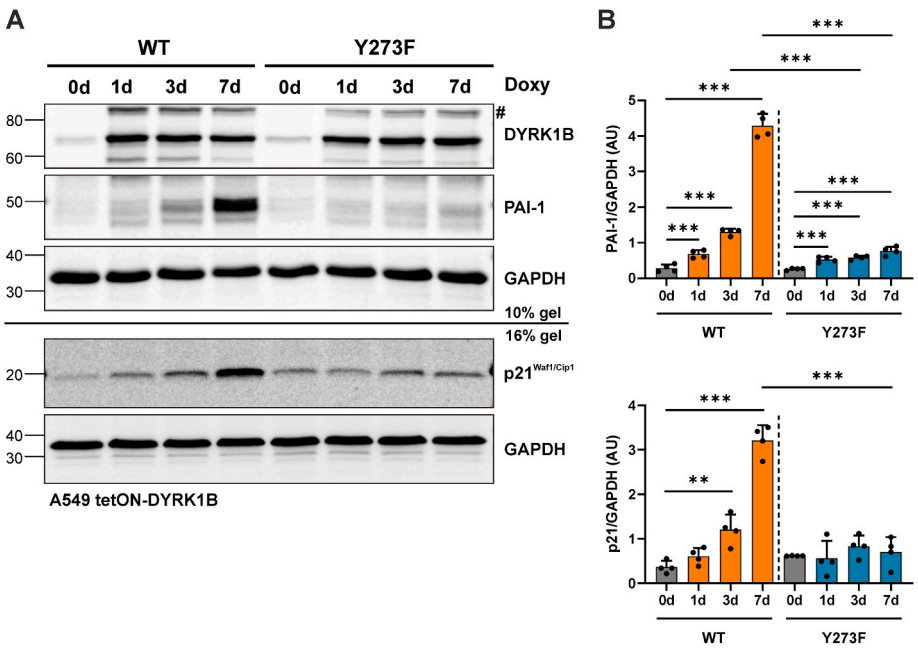


Fig. 2. Western blot analysis of PAI-1 and p21$^{Waf1/Cip1}$. A549-tetON cells were cultured for seven days, and overexpression of DYRK1B^{WT} or DYRK1B^{Y273F} was induced for 1–7 days using 2 μg/ml doxycycline. Aliquots of total cell lysates were subjected to Western blot analysis on two parallel gels (10% and 16% polyacrylamide) for successive immunodetection of the indicated proteins. GAPDH served as a loading control. The band marked by the hashtag (#) corresponds to the incompletely cleaved GFP-T2A-DYRK1B fusion protein. **A**, Representative Western blots. Migration of molecular weight standards is indicated in kDa (left). **B**, Densitometric analysis (mean ± SD) of n = 4 independent experiments. AU, arbitrary units. Statistical differences compared to the control are indicated by asterisks (*$p < 0.05$, **$p < 0.01$, ***$p < 0.001$).

in cell morphology and cytoplasmic granularity (b) increased levels of SA-β-gal, (c) transcriptional reprogramming that overlaps with established senescence-associated gene expression profiles, and (d) acquisition of a senescence-associated secretory phenotype (SASP).

How can the present findings be reconciled with our previous observations that DYRK1B overexpressing A549 cells develop mesenchymal traits, including morphological alterations, loss of cell-cell contacts, changes in the actin cytoskeleton, and increased migratory capacity? Moreover, we had shown that DYRK1B overexpression led to the upregulation of the canonical EMT transcription factors SNAIL, SLUG, and ZEB2 [13], among 15 EMT-related mRNAs that showed a >4-fold upregulation. Global transcriptome analysis in the present study confirms the upregulation of 14 out of these top 15 EMT-related genes. Additionally, four of the 20 most significantly upregulated genes in the present dataset (MT2A, PLAU, CDKN1A, and TGFB1, Fig. 4F) are included in the list of EMT signature genes compiled by Cook and Vanderheyden [41], based on their upregulation across diverse experimental EMT models.

Furthermore, it is important to acknowledge that the interplay between mesenchymal plasticity and stress-induced cellular senescence is highly context-dependent. While our findings characterize these dynamics within an epithelial carcinoma model undergoing EMT-like changes, recent studies in primary mesenchymal and stromal contexts—such as adipose, bone marrow, or amniotic stem cells—demonstrate that susceptibility to stress and the resulting microenvironmental senescence profiles are profoundly cell-type specific [42 43].

The transcriptome analysis also revealed extensive mRNA changes that closely align with senescence-associated gene expression signatures cataloged in the CellAge database, which are derived from both primary human cells and cancer cell lines [35]. Notably, several genes have been associated with both senescence and EMT. For example, *SERPINE1* (encoding PAI-1) is not only a well-established marker of cellular senescence [44 45 27] but also recognized as a mesenchymal marker in EMT analysis [46 47]. Similarly, *TGFB1* has been reported to promote cancer cell senescence in lung tumors [48] and is also known as a potent inducer of EMT [41]. Interestingly, a recent report showed that a subpopulation of MDA-MB 231 breast cancer cells exhibiting a more mesenchymal phenotype also displays elevated levels of senescence marker, thus providing evidence for a hybrid mesenchymal–senescent phenotype [49]. EMT and senescence traits were also correlated in human mammary epithelial cell (HMEC) cultures upon treatment with TGFβ [50].

The secretome of senescent cancer cells significantly reshapes the tumor microenvironment through paracrine effects, promoting migration, invasion, chronic inflammation, immune evasion, and EMT [51 52 53 54 55 56 57 58]. Thus, the mesenchymal features observed in DYRK1B-overexpressing A549 cells may represent a secondary effect of senescence induction (e.g. mediated via PAI-1 and TGFβ). Conversely, other studies have shown that an EMT-like transcriptomic program precedes senescence in etoposide-treated human IMR-90 cells [59]. However, because our current data rely on bulk population analyses, it remains to be determined whether these mesenchymal traits and senescence markers co-occur within individual cells—representing a true hybrid state—or if they reflect distinct subpopulations within the culture. Future single-cell resolution studies, such as single-cell RNA sequencing or dual-marker immunofluorescence, are needed to definitively dissect these two possibilities.

Either way, our characterization of DYRK1B-overexpressing A549 cells identifies DYRK1B as a pleiotropic mediator of phenotypic plasticity in vitro. Unlocking phenotypic plasticity, defined as the ability of cells to adapt to environmental challenges without genetic alterations, is recognized as a hallmark of cancer [14]. Notably, DYRK1B expression is upregulated in response to various environmental cues, including high cell density, serum deprivation, and hypoxia [60 61 62 11]. Extrapolating from these cellular data, we hypothesize that DYRK1B activation could represent an in vivo mechanism facilitating pro-tumorigenic adaptations that enhance tumor survival and therapy

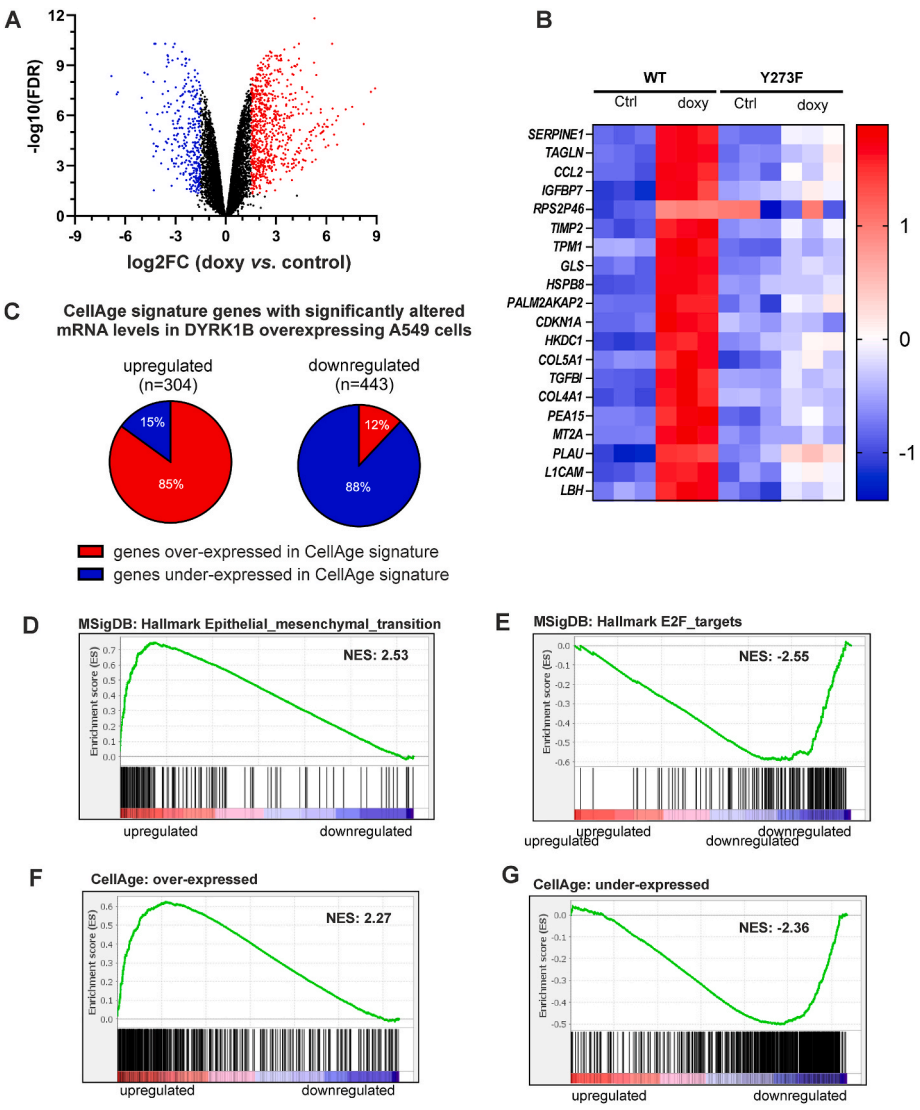


Fig. 3. Transcriptomic changes upon long-term overexpression of DYRK1B. A549 tetON DYRK1B-WT cells were cultured for seven days with doxycycline to induce overexpression of DYRK1B or remained untreated (n = 3). **A**, Volcano plot showing the distribution of gene expression fold changes and false discovery rates (FDR) of 12,720 genes. Significantly upregulated (red) or downregulated (blue) genes (FDR < 0.05 with a Log2 fold change >1.5) are highlighted. Selected senescence biomarkers are labeled. B, Heatmap showing the expression (Z-scores) of the top 20 significantly upregulated genes in overexpression compared to parallel samples overexpressing DYRK1B-Y273 F C, Comparison with the cellular senescence reference dataset obtained from CellAge [35,36]). Genes significantly up- or downregulated (FDR < 0.05) in A549 cells were assessed for their classification as over- or underexpressed in cellular senescence within the CellAge database **D** and **E**, Gene Set Enrichment Analysis (GSEA) using the Molecular Signatures Database (MSigDB). The enrichment plots illustrate the enrichment of (D) EMT genes among DYRK1B-upregulated genes and (E) E2F target genes among DYRK1B-downregulated genes. Normalized enrichment scores (NES) are indicated **F** and **G,** GSEA using the CellAge signature gene lists for genes that are (F) overexpressed or (G) underexpressed in cellular senescence. FDR q values for significant enrichment in D-G were <0.001. (For interpretation of the references to colour in this figure legend, the reader is referred to the Web version of this article.)

resistance—a premise that will require formal validation in future animal models.

Interestingly, recent evidence implicates DYRK1B in immune evasion. In a pancreatic cancer model, DYRK1B was shown to suppress tumoricidal macrophage activity by remodeling the tumor cell secretome [63]. In parallel, recent findings indicate that the closely related kinase DYRK1A also modulates the secretome of PANC-1 pancreatic adenocarcinoma cells to promote an immunosuppressive tumor microenvironment [64]. In this model, knockout of DYRK1A resulted in reduced expression of CCL-2, whereas knockout of DYRK1B produced the opposite effect. Overall, the relative contributions of DYRK1A and DYRK1B to immune regulation in pancreatic cancer and in other tumor types contexts appear to be highly context-dependent and warrant further investigation.

Our observation that DYRK1B induces features of cellular senescence is currently confined to a single clonal cancer cell line studied under in vitro conditions and involves levels of DYRK1B overexpression that likely exceed (patho-) physiological expression ranges. Notably, DYRK1B has independently been identified as a mediator of senescence in endothelial cells [18]. In addition, DYRK1A has been implicated in senescence induction through regulation of the DREAM complex, a key transcriptional regulator that enforces cell cycle exit [19,20]. Several studies further associate DYRK1A with aging-related processes involving cellular senescence [65 66 67]. Collectively, these findings suggest that DYRK1A and DYRK1B may share a conserved role in the regulation of cellular senescence.

What mechanism underlies the induction of senescence-associated features by DYRK1B in A549 cells? Sustained upregulation of CDK

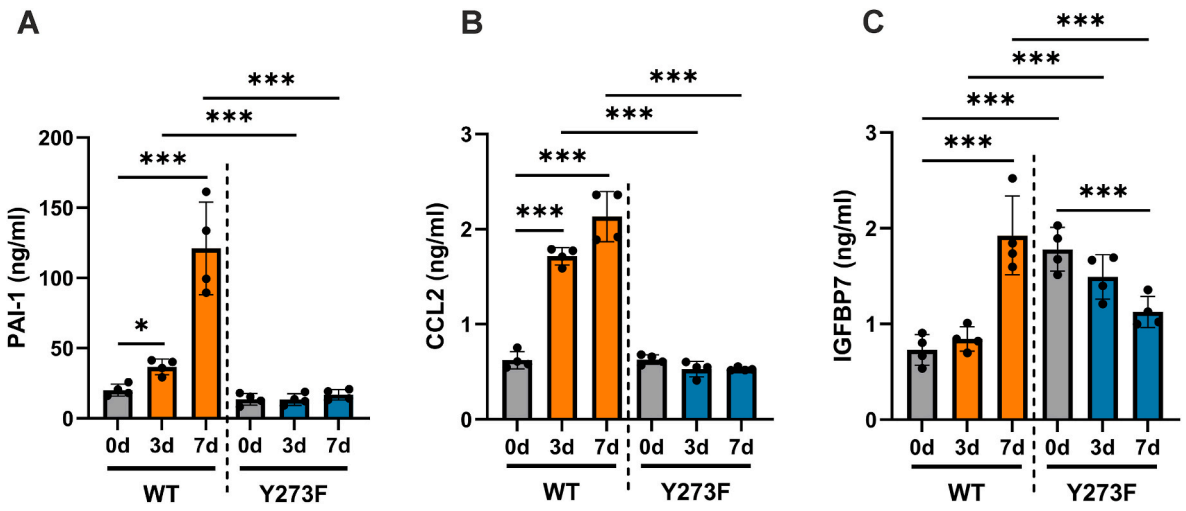


Fig. 4. DYRK1B overexpression drives secretion of SASP factors. Conditioned media were collected from A549 tetON cells after overexpression of $DYRK1B^{WT}$ or $DYRK1B^{Y273F}$ was induced for 3–7 days, using the same cultures as in the Western blot analysis shown in Fig. 2. Secreted factors were allowed to accumulate for 3 days before cell culture supernatants were analyzed by ELISA. Quantitative data of PAI-1 (A), CCL2 (B), and IGFBP7 (C) are shown as means ± SD of n = 4 independent experiments. *p < 0.05, **p < 0.01, ***p < 0.001.

inhibitors p21 or $p16^{Ink4a}$ is a key mechanism enforcing stable cell cycle arrest characteristic of senescent cells [68 55]. A549 cell harbor a homozygous deletion of the *CDKN2A* gene, which encodes $p16^{Ink4a}$, rendering this pathway inactive [69]. However, DYRK1B overexpression led to a progressive increase of p21 (encoded by *CDKN1A*) protein levels over a 7 day-period (Fig. 2). Notably, overexpression of p21 alone has been shown to be sufficient to induce senescence in tumor cells [70], and several models of p16-independent senescence induction have been reported [71]. p21 is also a central mediator of therapy-induced senescence, particularly in response to DNA damage caused by anticancer agents or radiation therapy [72 73]. Importantly, sustained p21 induction - such as that achieved by nutlin-3a–mediated p53 activation - can trigger senescence even in the absence of DNA damage [73]. Consistent with this model, DYRK1B-induced upregulation of p21 occurs without exogenous stress stimuli, suggesting that elevated DYRK1B levels may initiate a senescence program through direct or indirect upregulation of *CDKN1A* expression.

Taken together, our findings demonstrate that elevated levels of catalytically active DYRK1B in A549 cells induce phenotypic changes and transcriptional reprogramming that overlap with canonical hallmarks of cellular senescence. This suggests that DYRK1B upregulation in human cancers may contribute to remodeling the tumor microenvironment, thereby creating a “safe haven” that supports cancer cell survival and persistence [7]. Notably, pharmacological inhibition of DYRK1 has been used to achieve senolytic effects in cultured endothelial cells through targeting DYRK1B [18] and to correct senescence-associated processes via inhibition of DYRK1A [65 67 74]. Future studies will be required to explore the effects of DYRK1B inhibition on cancer cell senescence.

5. Conclusions

Our findings position DYRK1B as a pleiotropic regulator of cancer cell phenotypic plasticity. The coexistence of senescence- and EMT-associated transcriptional programs suggests that DYRK1B may promote hybrid or heterogeneous cell states with potential relevance for microenvironmental modulation and therapy resistance. While the present study is limited to an in vitro overexpression model, the convergence of our data with emerging evidence from other cell types and systems supports a broader role for DYRK1B in the regulation of senescence-associated processes. Together, these results highlight DYRK1B as a candidate molecular node connecting stress adaptation, senescence, and tumor cell survival, and provide a rationale for future studies addressing the context-dependent roles of DYRK1B in cancer progression and its potential as a therapeutic target to modulate senescence-associated phenotypes.

CRediT authorship contribution statement

Gerrit Wilms: Visualization, Methodology, Investigation, Funding acquisition, Formal analysis, Data curation. **Aaron Babendreyer:** Resources, Investigation. **Justyna Wozniak:** Formal analysis, Data curation. **Florian Kraft:** Visualization, Resources, Investigation, Data curation. **Walter Becker:** Writing – review & editing, Writing – original draft, Project administration, Funding acquisition, Conceptualization.

Availability of data and materials

The RNA-seq datasets have been deposited in NCBI's Gene Expression Omnibus and are accessible through GEO Series accession number GSE326699. The ranked list of gene expression changes is provided in the supplementary material.

Authors' contributions

GW designed and performed the majority of experiments, analyzed the data, and coordinated the collaborative work. GW and AB conducted the flow cytometry experiments. GW and FK designed and carried out the RNA-seq experiments and performed the associated data analysis. GW and JW performed the statistical analyses. GW and WB conceived the study, supervised the experimental work, interpreted the data, and wrote the manuscript. All authors reviewed, provided critical feedback on, and approved the final version of the manuscript.

Declaration of generative AI and AI-assisted technologies in the manuscript preparation process

WB used ChatGPT for improving the language accuracy and readability of the text. After using this tool, the authors reviewed the manuscript and take full responsibility for the final version of the article.

Funding

This work was supported by the German Research Foundation (DFG) projects 424656244 and 520339551 (BE 1967/5-1 and BE 1967/6-1, to WB), and by the START-Program of the Faculty of Medicine of the RWTH Aachen University (Innenauftragsnummer 692214, Az 20/22, to GW).

Declaration of competing interest

The authors declare the following financial interests/personal relationships which may be considered as potential competing interests: GW and WB are co-inventors of patents on DYRK PROTACs (PCT/US2023/080099 and PCT/US2024/050636).

Acknowledgements

We thank Sebastian Giesselmann for excellent technical assistance with the RNA-seq experiments.

List of abbreviations:

EMT, epithelial mesenchymal transition; FACS, fluorescence-activated cell sorting; FDR, false discovery rate; FSC, forward scatter; GFP, green fluorescent protein; GSEA, gene set enrichment analysis; log_2FC, log_2 fold change; SA-β-gal, senescence-associated β-galactosidase; SASP, senescence-associated secretory phenotype; SSC, side scatter.

Appendix A. Supplementary data

Supplementary data to this article can be found online at https://doi.org/10.1016/j.bbrc.2026.154685.

References

[1] S. Aranda, A. Laguna, S. de la Luna, DYRK family of protein kinases: evolutionary relationships, biochemical properties, and functional roles, FASEB J. 25 (2) (2011) 449–462, https://doi.org/10.1096/fj.10-165837. PMID: 21048044.
[2] L. Suanes-Cobos, M. Torres-Ramos, I. Aguilera-Ventura, A. Serrano-Yubero, M. A. Calzado, The dual fate of DYRK2 in cancer: balancing the light and dark side of tumorigenesis, Cancer Metastasis Rev. 45 (1) (2026) 2, https://doi.org/10.1007/s10555-025-10311-0. PMID: 41524942.
[3] U. Soppa, W. Becker, DYRK protein kinases, Curr. Biol. 25 (12) (2015) R488–R489, https://doi.org/10.1016/j.cub.2015.02.067. PMID: 26079075.
[4] J. Boni, C. Rubio-Perez, N. López-Bigas, C. Fillat, S. de la Luna, The DYRK family of kinases in cancer: molecular functions and therapeutic opportunities, Cancers (Basel) 12 (8) (2020) 2106, https://doi.org/10.3390/cancers12082106. PMID: 32751160.
[5] W. Becker, A wake-up call to quiescent cancer cells - potential use of DYRK1B inhibitors in cancer therapy, FEBS J. 285 (7) (2018) 1203–1211, https://doi.org/10.1111/febs.14347. PMID: 29193696.
[6] N. Kokkorakis, M. Zouridakis, M. Gaitanou, Mirk/Dyrk1B kinase inhibitors in targeted cancer therapy, Pharmaceutics 16 (4) (2024) 528, https://doi.org/10.3390/pharmaceutics16040528. PMID: 38675189.
[7] M. Ems, A. Brichkina, M. Lauth, A safe haven for cancer cells: tumor plus stroma control by DYRK1B, Oncogene 44 (6) (2025) 341–347, https://doi.org/10.1038/s41388-025-03275-6. PMID: 39863750.
[8] D.Z. Ewton, K. Lee, X. Deng, S. Lim, E. Friedman, Rapid turnover of cell-cycle regulators found in Mirk/dyrk1B transfectants, Int. J. Cancer 103 (1) (2003) 21–28, https://doi.org/10.1002/ijc.10743. PMID: 12455049.
[9] X. Deng, S.E. Mercer, S. Shah, D.Z. Ewton, E. Friedman, The cyclin-dependent kinase inhibitor p27Kip1 is stabilized in G(0) by Mirk/dyrk1B kinase, J. Biol. Chem. 279 (21) (2004) 22498–22504, https://doi.org/10.1074/jbc.M400479200. PMID: 15010468.
[10] X. Deng, D.Z. Ewton, E. Friedman, Mirk/Dyrk1B maintains the viability of quiescent pancreatic cancer cells by reducing levels of reactive oxygen species, Cancer Res. 69 (8) (2009) 3317–3324, https://doi.org/10.1158/0008-5472.CAN-08-2903. PMID: 19351855.
[11] C. Beckers, L. Vasilikos, A. Sanchez Fernandez, L. Moor, M. Pruschy, Targeting the survival kinase DYRK1B: a novel approach to overcome radiotherapy-related treatment resistance, Radiother. Oncol. 190 (2024) 110039, https://doi.org/10.1016/j.radonc.2023.110039. PMID: 38040123.
[12] C. Dong, K.L. West, X.Y. Tan, J. Li, T. Ishibashi, C.H. Yu, S.M.H. Sy, J.W.C. Leung, M.S.Y. Huen, Screen identifies DYRK1B network as mediator of transcription repression on damaged chromatin, Proc. Natl. Acad. Sci. USA 117 (29) (2020) 17019–17030, https://doi.org/10.1073/pnas.2002193117. PMID: 32611815.
[13] S. Sester, G. Wilms, J. Ahlburg, A. Babendreyer, W. Becker, Elevated expression levels of the protein kinase DYRK1B induce mesenchymal features in A549 lung cancer cells, BMC Cancer 24 (1) (2024 Oct 31) 1341, https://doi.org/10.1186/s12885-024-13057-0. PMID: 39482615.
[14] D. Hanahan, Hallmarks of cancer: new dimensions, Cancer Discov. 12 (1) (2022) 31–46, https://doi.org/10.1158/2159-8290.CD-21-1059. PMID: 35022204.
[15] R. Fontana, A. Mestre-Farrera, J. Yang, Update on epithelial-mesenchymal plasticity in cancer progression, Annu. Rev. Pathol. 19 (2024) 133–156, https://doi.org/10.1146/annurev-pathmechdis-051222-122423. PMID: 37758242.
[16] F. d'Adda di Fagagna, Living on a break: cellular senescence as a DNA-damage response, Nat. Rev. Cancer 8 (7) (2008) 512–522, https://doi.org/10.1038/nrc2440. PMID: 18574463.
[17] D. McHugh, I. Durán, J. Gil, Senescence as a therapeutic target in cancer and age-related diseases, Nat. Rev. Drug Discov. 24 (1) (2025) 57–71, https://doi.org/10.1038/s41573-024-01074-4. PMID: 39548312.
[18] F.M. Pramotton, A. Abukar, C. Hudson, J. Dunbar, A. Potterton, S. Tonnicchia, A. Taddei, E. Mazza, C. Giampietro, DYRK1B inhibition exerts senolytic effects on endothelial cells and rescues endothelial dysfunctions, Mech. Ageing Dev. 213 (2023) 111836, https://doi.org/10.1016/j.mad.2023.111836. PMID: 37301518.
[19] L. Litovchick, L.A. Florens, S.K. Swanson, M.P. Washburn, J.A. DeCaprio, DYRK1A protein kinase promotes quiescence and senescence through DREAM complex assembly, Genes Dev. 25 (8) (2011) 801–813, https://doi.org/10.1101/gad.2034211. PMID: 21498570.
[20] G.A. Roozbahani, M.H. Horestani, K. Schindler, J. Kallenbach, A. Baniahmad, Induction of cellular senescence by androgen receptor agonist or antagonist is mediated via two novel common DYRK1A-DREAM and cyclin G2 signaling pathways in castration-resistant prostate cancer, J. Adv. Res. 80 (2026) 371–392, https://doi.org/10.1016/j.jare.2025.05.019. PMID: 40368177.
[21] A. Degasperi, M.R. Birtwistle, N. Volinsky, J. Rauch, W. Kolch, B.N. Kholodenko, Evaluating strategies to normalise biological replicates of Western blot data, PLoS One 9 (2014) e87293.
[22] A. Dobin, C.A. Davis, F. Schlesinger, J. Drenkow, C. Zaleski, S. Jha, P. Batut, M. Chaisson, T.R. Gingeras, STAR: ultrafast universal RNA-seq aligner, Bioinformatics 29 (1) (2013) 15–21, https://doi.org/10.1093/bioinformatics/bts635.
[23] D. Torre, A. Lachmann, A. Ma'ayan, BioJupies: automated generation of interactive notebooks for RNA-Seq data analysis in the cloud, Cell Syst. 7 (5) (2018) 556–561. e3, https://doi.org/10.1016/j.cels.2018.10.007.
[24] M.E. Ritchie, B. Phipson, D. Wu, Y. Hu, C.W. Law, W. Shi, G.K. Smyth, Limma powers differential expression analyses for RNA-sequencing and microarray studies, Nucleic Acids Res. 43 (7) (2015) e47.
[25] A. Subramanian, P. Tamayo, V.K. Mootha, S. Mukherjee, B.L. Ebert, M.A. Gillette, A. Paulovich, S.L. Pomeroy, T.R. Golub, E.S. Lander, J.P. Mesirov, Gene set enrichment analysis: a knowledge-based approach for interpreting genome-wide expression profiles, Proc. Natl. Acad. Sci. U. S. A. 102 (43) (2005) 15545–15550, https://doi.org/10.1073/pnas.0506580102. PMID: 16199517.
[26] A. Liberzon, C. Birger, H. Thorvaldsdóttir, M. Ghandi, J.P. Mesirov, P. Tamayo, The Molecular Signatures Database (MSigDB) hallmark gene set collection, Cell Syst. 1 (6) (2015) 417–425, https://doi.org/10.1016/j.cels.2015.12.004. PMID: 26771021.
[27] E. González-Gualda, A.G. Baker, L. Fruk, D. Muñoz-Espín, A guide to assessing cellular senescence in vitro and in vivo, FEBS J. 288 (1) (2021) 56–80, https://doi.org/10.1111/febs.15570. PMID: 32961620.
[28] A. Litwiniec, A. Grzanka, A. Helmin-Basa, L. Gackowska, D. Grzanka, Features of senescence and cell death induced by doxorubicin in A549 cells: organization and level of selected cytoskeletal proteins, J. Cancer Res. Clin. Oncol. 136 (5) (2010) 717–736, https://doi.org/10.1007/s00432-009-0711-4. PMID: 19898866.
[29] N. Wiesmann, R. Gieringer, M. Viel, J. Eckrich, W. Tremel, J. Brieger, Zinc oxide nanoparticles can intervene in radiation-induced senescence and eradicate residual tumor cells, Cancers (Basel) 13 (12) (2021) 2989, https://doi.org/10.3390/cancers13122989. PMID: 34203835.
[30] L. Yang, J. Fang, J. Chen, Tumor cell senescence response produces aggressive variants, Cell Death Discov. 3 (2017) 17049, https://doi.org/10.1038/cddiscovery.2017.49. PMID: 28845296.
[31] E. Goy, N. Martin, C. Drullion, L. Saas, O. Molendi-Coste, L. Pineau, D. Dombrowicz, E. Deruy, H. Bauderlique-Le-Roy, O. Samyn, Y. De Launoit, C. Abbadie, Flow cytometry-based method for efficient sorting of senescent cells, Bio Protoc 13 (7) (2023) e4612, https://doi.org/10.21769/BioProtoc.4612.
[32] Jhaisha S. Abu, E.W. Widowati, I. Kii, R. Sonamoto, S. Knapp, C. Papadopoulos, W. Becker, DYRK1B mutations associated with metabolic syndrome impair the chaperone-dependent maturation of the kinase domain, Sci. Rep. 7 (1) (2017) 6420, https://doi.org/10.1038/s41598-017-06874-w. PMID: 28743892.
[33] R.M. Kortlever, P.J. Higgins, R. Bernards, Plasminogen activator inhibitor-1 is a critical downstream target of p53 in the induction of replicative senescence, Nat. Cell Biol. 8 (8) (2006) 877–884, https://doi.org/10.1038/ncb1448.
[34] M. Eren, A.E. Boe, S.B. Murphy, A.T. Place, V. Nagpal, L. Morales-Nebreda, et al., PAI-1-regulated extracellular proteolysis governs senescence and survival in Klotho mice, Proc. Natl. Acad. Sci. U. S. A. 111 (19) (2014) 7090–7095, https://doi.org/10.1073/pnas.1321942111.
[35] R.A. Avelar, J.G. Ortega, R. Tacutu, E.J. Tyler, D. Bennett, P. Binetti, et al., A multidimensional systems biology analysis of cellular senescence in aging and disease, Genome Biol. 21 (1) (2020) 91, https://doi.org/10.1186/s13059-020-01990-9. PMID: 32264951.

[36] K. Chatsirisupachai, D. Palmer, S. Ferreira, J.P. de Magalhães, A human tissue-specific transcriptomic analysis reveals a complex relationship between aging, cancer, and cellular senescence, Aging Cell 18 (6) (2019) e13041, https://doi.org/10.1111/acel.13041. PMID: 31560156.
[37] A.L. Fridman, M.A. Tainsky, Critical pathways in cellular senescence and immortalization revealed by gene expression profiling, Oncogene 27 (46) (2008) 5975–5987, https://doi.org/10.1038/onc.2008.213. PMID: 18711403.
[38] D. Saul, R.L. Kosinsky, E.J. Atkinson, M.L. Doolittle, X. Zhang, N.K. LeBrasseur, et al., A new gene set identifies senescent cells and predicts senescence-associated pathways across tissues, Nat. Commun. 13 (1) (2022) 4827, https://doi.org/10.1038/s41467-022-32552-1. PMID: 35974106.
[39] B. Fernandez, V.J. Passanisi, H.M. Ashraf, S.L. Spencer, Single-cell RNA sequencing reveals a quiescence-senescence continuum and distinct senotypes following chemotherapy, Nat. Commun. 17 (1) (2025) 169, https://doi.org/10.1038/s41467-025-66836-z. PMID: 41436452.
[40] A. Hernandez-Segura, J. Nehme, M. Demaria, Hallmarks of cellular senescence, Trends Cell Biol. 28 (6) (2018) 436–453, https://doi.org/10.1016/j.tcb.2018.02.001. PMID: 29477613.
[41] D.P. Cook, B.C. Vanderhyden, Context specificity of the EMT transcriptional response, Nat. Commun. 11 (1) (2020) 2142, https://doi.org/10.1038/s41467-020-16066-2. PMID: 32358524.
[42] N. Alessio, M.B. Acar, I.H. Demirsoy, T. Squillaro, D. Siniscalco, G. Di Bernardo, G. Peluso, S. Özcan, U. Galderisi, Obesity is associated with senescence of mesenchymal stromal cells derived from bone marrow, subcutaneous and visceral fat of young mice, Aging (Albany NY) 12 (13) (2020) 12609–12621, https://doi.org/10.18632/aging.103606. PMID: 32634118.
[43] N. Alessio, C. Pipino, D. Mandatori, P. Di Tomo, A. Ferone, M. Marchiso, M.A. B. Melone, G. Peluso, A. Pandolfi, U. Galderisi, Mesenchymal stromal cells from amniotic fluid are less prone to senescence compared to those obtained from bone marrow: an in vitro study, J. Cell. Physiol. 233 (11) (2018) 8996–9006, https://doi.org/10.1002/jcp.26845. PMID: 29904927.
[44] R.M. Kortlever, P.J. Higgins, R. Bernards, Plasminogen activator inhibitor-1 is a critical downstream target of p53 in the induction of replicative senescence, Nat. Cell Biol. 8 (2006) 877–884.
[45] D.E. Vaughan, R. Rai, S.S. Khan, M. Eren, A.K. Ghosh, Plasminogen activator Inhibitor-1 is a marker and a mediator of senescence, Arterioscler. Thromb. Vasc. Biol. 37 (8) (2017) 1446–1452, https://doi.org/10.1161/ATVBAHA.117.309451. PMID: 28572158.
[46] W. Dai, Y. Xiao, W. Tang, J. Li, L. Hong, J. Zhang, M. Pei, J. Lin, S. Liu, X. Wu, L. Xiang, J. Wang, Identification of an EMT-Related gene signature for predicting overall survival in gastric cancer, Front. Genet. 12 (2021) 661306, https://doi.org/10.3389/fgene.2021.661306. PMID: 34249086.
[47] H.J. Kong, E.J. Kwon, O.S. Kwon, H. Lee, J.Y. Choi, Y.J. Kim, W. Kim, H.J. Cha, Crosstalk between YAP and TGFβ regulates SERPINE1 expression in mesenchymal lung cancer cells, Int. J. Oncol. 58 (1) (2021) 111–121, https://doi.org/10.3892/ijo.2020.5153. PMID: 33367928.
[48] S. Matsuda, A. Revandkar, T.D. Dubash, A. Ravi, B.S. Wittner, M. Lin, R. Morris, R. Burr, H. Guo, K. Seeger, A. Szabolcs, D. Che, L. Nieman, G.A. Getz, D.T. Ting, M. S. Lawrence, J. Gainor, D.A. Haber, S. Maheswaran, TGF-β in the microenvironment induces a physiologically occurring immune-suppressive senescent state, Cell Rep. 42 (3) (2023) 112129, https://doi.org/10.1016/j.celrep.2023.112129. PMID: 36821441.
[49] Murillo L. Larrea, C.J. Sugden, B. Ozsvari, Z. Moftakhar, G.S. Hassan, F. Sotgia, M. P. Lisanti, ALDHHigh breast cancer stem cells exhibit a mesenchymal-senescent hybrid phenotype, with elevated metabolic and migratory activities, Cells 13 (24) (2024) 2059, https://doi.org/10.3390/cells13242059. PMID: 39768151.
[50] J.A. Caruso, C. Chen-Tanyolac, T.D. Tlsty, A hybrid epithelial-mesenchymal transition program enables basal epithelial cells to bypass stress-induced stasis and contributes to a metaplastic breast cancer progenitor state, Breast Cancer Res. 26 (1) (2024) 184, https://doi.org/10.1186/s13058-024-01920-8. PMID: 39696672.
[51] A. Freund, A.V. Orjalo, P.Y. Desprez, J. Campisi, Inflammatory networks during cellular senescence: causes and consequences, Trends Mol. Med. 16 (5) (2010) 238–246, https://doi.org/10.1016/j.molmed.2010.03.003. PMID: 20444648.
[52] R.M. Laberge, P. Awad, J. Campisi, P.Y. Desprez, Epithelial-mesenchymal transition induced by senescent fibroblasts, Cancer Microenviron 5 (1) (2012) 39–44, https://doi.org/10.1007/s12307-011-0069-4. PMID: 21706180.
[53] P. Lecot, F. Alimirah, P.Y. Desprez, J. Campisi, C. Wiley, Context-dependent effects of cellular senescence in cancer development, Br. J. Cancer 114 (11) (2016) 1180–1184, https://doi.org/10.1038/bjc.2016.115. PMID: 27140310.
[54] N. Wajapeyee, R.W. Serra, X. Zhu, M. Mahalingam, M.R. Green, Oncogenic BRAF induces senescence and apoptosis through pathways mediated by the secreted protein IGFBP7, Cell 132 (2008) 363–374.
[55] M. Takasugi, Y. Yoshida, E. Hara, N. Ohtani, The role of cellular senescence and SASP in tumour microenvironment, FEBS J. 290 (5) (2023) 1348–1361, https://doi.org/10.1111/febs.16381. PMID: 35106956.
[56] N. Levi, N. Papismadov, I. Solomonov, I. Sagi, V. Krizhanovsky, The ECM path of senescence in aging: components and modifiers, FEBS J. 287 (13) (2020) 2636–2646, https://doi.org/10.1111/febs.15282. PMID: 32145148.
[57] M.M. Faheem, N.D. Seligson, S.M. Ahmad, R.U. Rasool, S.G. Gandhi, M. Bhagat, A. Goswami, Convergence of therapy-induced senescence (TIS) and EMT in multistep carcinogenesis: current opinions and emerging perspectives, Cell Death Discov. 6 (2020) 51, https://doi.org/10.1038/s41420-020-0286-z. PMID: 32566256.
[58] B. Wang, J. Han, J.H. Elisseeff, M. Demaria, The senescence-associated secretory phenotype and its physiological and pathological implications, Nat. Rev. Mol. Cell Biol. 25 (12) (2024) 958–978, https://doi.org/10.1038/s41580-024-00727-x. PMID: 38654098. x.
[59] C. Anerillas, A.B. Herman, M. Rossi, R. Munk, E. Lehrmann, J.L. Martindale, C. Y. Cui, K. Abdelmohsen, S. De, M. Gorospe, Early SRC activation skews cell fate from apoptosis to senescence, Sci. Adv. 8 (14) (2022) eabm0756, https://doi.org/10.1126/sciadv.abm0756. PMID: 35394839.
[60] K. Jin, D.Z. Ewton, S. Park, J. Hu, E. Friedman, Mirk regulates the exit of colon cancer cells from quiescence, J. Biol. Chem. 284 (34) (2009) 22916–22925, https://doi.org/10.1074/jbc.M109.035519. PMID: 19542220.
[61] A.J. Massey, K. Benwell, M. Burbridge, A. Kotschy, D.L. Walmsley, Targeting DYRK1A/B kinases to modulate p21-cyclin D1-p27 signalling and induce anti-tumour activity in a model of human glioblastoma, J. Cell Mol. Med. 25 (22) (2021) 10650–10662, https://doi.org/10.1111/jcmm.17002. PMID: 34708541.
[62] V.A. Vorwerk, G. Wilms, A. Babendreyer, W. Becker, Differential regulation of expression of the protein kinases DYRK1A and DYRK1B in cancer cells, Sci. Rep. 14 (1) (2024) 23926, https://doi.org/10.1038/s41598-024-74190-1. PMID: 39397076.
[63] A. Brichkina, M. Ems, R. Suezov, R. Singh, V. Lutz, F.S.R. Picard, A. Nist, T. Stiewe, J. Graumann, M. Daude, W.E. Diederich, F. Finkernagel, H.R. Chung, D.K. Bartsch, K. Roth, C. Keber, C. Denkert, M. Huber, T.M. Gress, M. Lauth, DYRK1B blockade promotes tumoricidal macrophage activity in pancreatic cancer, Gut 73 (10) (2024) 1684–1701, https://doi.org/10.1136/gutjnl-2023-331854. PMID: 38834297.
[64] S. Pascual-Sabater, S. Varhadi, C. Di Vona, M. Celma, C. Fillat, S. de la Luna, DYRK1A regulates cancer cell and cancer-associated fibroblast secretomes to foster an immunosuppressive microenvironment in pancreatic cancer, bioRxiv 11.26 (2025) 690756, https://doi.org/10.1101/2025.11.26.690756.
[65] T. Kaise, M. Fukui, R. Sueda, W. Piao, M. Yamada, T. Kobayashi, I. Imayoshi, R. Kageyama, Functional rejuvenation of aged neural stem cells by Plagl2 and anti-Dyrk1a activity, Genes Dev. 36 (1–2) (2022) 23–37, https://doi.org/10.1101/gad.349000.121. Erratum in: Genes Dev. 2024;38(21-24):1047. doi: 10.1101/gad.352361.124. PMID: 34916302.
[66] A. Murray, G. Gough, A. Cindrić, F. Vučković, D. Koschut, V. Borelli, et al., Dose imbalance of DYRK1A kinase causes systemic progeroid status in Down syndrome by increasing the un-repaired DNA damage and reducing LaminB1 levels, EBioMedicine 94 (2023) 104692, https://doi.org/10.1016/j.ebiom.2023.104692. PMID: 37451904.
[67] A. Bujarrabal-Dueso, G. Sendtner, D.H. Meyer, G. Chatzinikolaou, K. Stratigi, G. A. Garinis, B. Schumacher, The DREAM complex functions as conserved master regulator of somatic DNA-repair capacities, Nat. Struct. Mol. Biol. 30 (4) (2023) 475–488, https://doi.org/10.1038/s41594-023-00942-8. PMID: 36959262.
[68] J. Mikuła-Pietrasik, A. Niklas, P. Uruski, A. Tykarski, K. Książek, Mechanisms and significance of therapy-induced and spontaneous senescence of cancer cells, Cell. Mol. Life Sci. 77 (2) (2020) 213–229, https://doi.org/10.1007/s00018-019-03261-8. PMID: 31414165.
[69] M.J. Park, K. Shimizu, T. Nakano, Y.B. Park, T. Kohno, M. Tani, J. Yokota, Pathogenetic and biologic significance of TP14ARF alterations in non small cell lung carcinoma, Cancer Genet. Cytogenet. 141 (1) (2003) 5–13, https://doi.org/10.1016/s0165-4608(02)00645-3. PMID: 12581892.
[70] L. Fang, M. Igarashi, J. Leung, M.M. Sugrue, S.W. Lee, S.A. Aaronson, p21Waf1/Cip1/Sdi1 induces permanent growth arrest with markers of replicative senescence in human tumor cells lacking functional p53, Oncogene 18 (18) (1999) 2789–2797, https://doi.org/10.1038/sj.onc.1202615. PMID: 10362249.
[71] Z. Liao, H.L. Yeo, S.W. Wong, Y. Zhao, Cellular senescence: mechanisms and therapeutic potential, Biomedicines 9 (12) (2021) 1769, https://doi.org/10.3390/biomedicines9121769. PMID: 34944585.
[72] I.B. Roninson, Tumor cell senescence in cancer treatment, Cancer Res. 63 (11) (2003) 2705–2715. PMID: 12782571.
[73] C.H. Hsu, S.J. Altschuler, L.F. Wu, Patterns of early p21 dynamics determine proliferation-senescence cell fate after chemotherapy, Cell 178 (2) (2019) 361–373.e12, https://doi.org/10.1016/j.cell.2019.05.041. PMID: 31204100.
[74] A. Murray, G. Gough, A. Cindrić, F. Vučković, D. Koschut, V. Borelli, et al., Dose imbalance of DYRK1A kinase causes systemic progeroid status in Down syndrome by increasing the un-repaired DNA damage and reducing LaminB1 levels, EBioMedicine 94 (2023) 104692, https://doi.org/10.1016/j.ebiom.2023.104692. PMID: 37451904.